Available online at www.sciencedirect.com
SCIENCE DIRECT®
Materials Chemistry and Physics 92 (2005) 48–53
MATERIALS CHEMISTRY AND PHYSICS
www.elsevier.com/locate/matchemphys

Microstructural investigation of hexagonal-shaped diamond nanoplatelets grown by microwave plasma chemical vapor deposition

Chun-An Lu*, Li Chang

Department of Materials Science and Engineering, National Chiao Tung University, Hsinchu 30010, Taiwan, ROC

Received 6 August 2004; received in revised form 23 December 2004; accepted 27 December 2004

Abstract

Diamond crystallites in hexagonal-shaped nanoplatelet morphology were synthesized in microwave plasma chemical vapor deposition (MPCVD) system using a CH_4/H_2 gas mixture with a ratio of 0.667%. Diamond nanoplatelets were deposited on (1 0 0) silicon substrate. The substrate was embedded within the plasma ball close to its center where the high temperature above 1100 °C was reached during the deposition. Surface morphologies and crystalline characteristics of the deposited diamond were examined by scanning electron microscopy (SEM) and transmission electron microscopy (TEM). SEM and TEM observations clearly show that the diamond nanoplatelets exhibit hexagonal-shaped morphologies, and the thickness and the length are measured to be around 20–30 nm and several hundred nanometers, respectively. Also, SEM shows that the distribution of the nanoplatelet density gradually increases from the center to the corner of the sample. TEM with selected area electron diffraction shows that each platelet is a single crystalline diamond. Both ⟨1 1 0⟩ and ⟨1 1 1⟩ orientations of the diamond platelets are observed.

Keywords: Platelets; Electron microscopy; Diffraction

1. Introduction

With the advent of nanotechnology related research in resent years, it is of increasing interests in studying nanostructured diamond [1–4]. Various forms of nanostructured diamond have been synthesized such as nanopowders [5] and nanocrystalline films [6–10]. Nanocrystalline diamond films have a great deal of particular properties, including smooth surfaces, the low friction coefficient, high thermal conductivity, wide band gap, high mobility of electrons and holes and low dielectric constant, which can be used in electronic, optical and mechanical applications. In this paper, we present an exceptional nanocrystalline diamond in platelet configuration of hexagonal shape. Although the platelet diamond with hexagonal structure synthesized at temperature around 850 °C has been reported [11], the linear dimension is much larger in micrometer scale. In addition, the formation of the diamond platelet with low aspect ratio has been shown to be accompanied with diamond crystallites with three-dimension faceting. Here we report that a large quantity of two-dimensional diamond nanoplatelets in an average thickness of about 25 nm with hexagonal shape were successfully synthesized by chemical vapor deposition (CVD) with the reaction gas composed of hydrogen and methane. The formation of diamond nanoplatelets demonstrates a new area of CVD diamond crystal growth unexplored before. The hexagonal shape diamond nanoplatelets were characterized by scanning electron microscopy (SEM) and transmission electron microscopy (TEM) with selected area diffraction (SAD).

2. Experimental

Nanocrystalline diamond platelets were synthesized in an ASTeX 2.45 GHz microwave plasma chemical deposition

* Corresponding author. Tel.: +886 35712121/55373; fax: +886 35724727.
E-mail address: chunanlu.mse88g@nctu.edu.tw (C.-A. Lu).

0254-0584/$ – see front matter © 2005 Elsevier B.V. All rights reserved.
doi:10.1016/j.matchemphys.2004.12.041

Table 1
Experimental parameters for synthesis of diamond nanoplatelets

Process	Time (min)	Pressure (Torr)	Gas flow rate (sccm)	Power (W)	Bias (V)
Reduction	10	20	H_2 300	800	
Nucleation	15	20	H_2/CH_4 = 288:12 (4%)	800	−200
Growth	30	20	H_2/CH_4 = 298:2 (0.667%)	800	

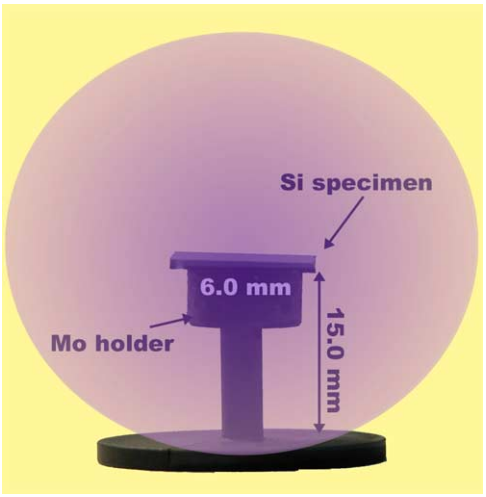

Fig. 1. Schematic diagram of arrangement of the substrate and the holder with respect to the plasma ball.

system. The 10.0 mm × 10.0 mm silicon (1 0 0) substrate was placed on a molybdenum holder which had been raised its height close to the center of the plasma ball, as schematically shown in Fig. 1. Such a configuration ensured that the plasma ball enclosed the whole set of the Mo holder and the substrate. The substrate temperature was above 1150 °C as measured by an optical pyrometer. The gas flow rates of CH_4 and H_2 were fixed at 2 and 298 sccm, respectively, and the process pressure was 20 Torr. The process parameters were summarized in Table 1. After deposition, the surface morphology was examined in a field-emission scanning electron microscope (JEOL JSM6500-F operated at 10 kV). Further microstructural characterization for detailed morphology and crystallography was carried out using a Philips Tecnai 20 transmission electron microscope. In the sample preparation for TEM, the specimens were immersed in an ethanol solution, followed by ultrasonic treatment to disperse diamond platelets. The diamond-dispersed solution was then dipped on a copper grid with a holey carbon film.

3. Results and discussion

3.1. Morphological characterization by scanning electron microscopy

Fig. 2 shows the surface morphology on different substrate areas after deposition. The surface morphology around the center of the substrate was shown in Fig. 2(a) and (b).

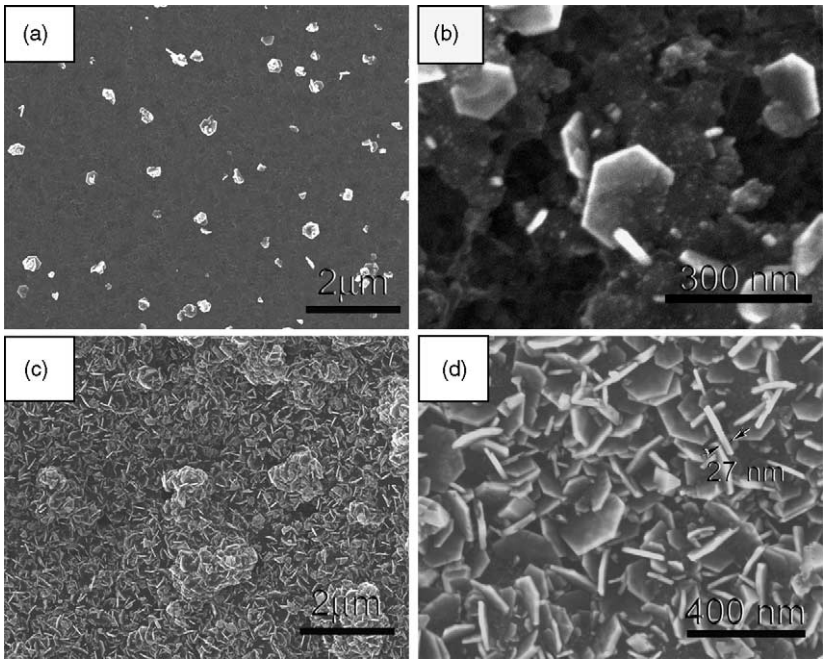

Fig. 2. SEM micrographs showing the surface morphology of (a) the center area of the substrate with high magnification in (b), and (c) the corner area with high magnification in (d).

Fig. 2(a) is a low-magnification SEM micrograph, showing that a small amount of the deposits of ~0.3 μm size in bright contrast are in a scattered distribution. In Fig. 2(b) of high-magnification micrograph of one deposit, we can see that it is a cluster of a large number of platelets which clearly exhibit a nearly hexagonal-shaped morphology. The measured thickness of the platelets is approximately 10–30 nm and the length is less than 200 nm. Some of nanoplatelets are seen to lie on the substrate surface and a few are standing almost vertically on it. Fig. 2(c) and (d) shows the morphology of the diamond around the corner areas of the substrate. A large quantity of interlaced nanoplatelets are found to be densely distributed over the corner areas of the specimen surface. The size of the nanoplatelets is similar to that in the central area (Fig. 2(b)). The distribution of nanoplatelet density around the corner area is estimated over 1×10^{10} cm^{-2}. It is observed that the distribution of crystalline diamond nanoplatelet is not uniform over the whole substrate surface from the center to the corner. The density gradually distribution increased from the center of the substrate surface to the corner. It is coincident with the measured temperature distribution on the surface of the substrate during the

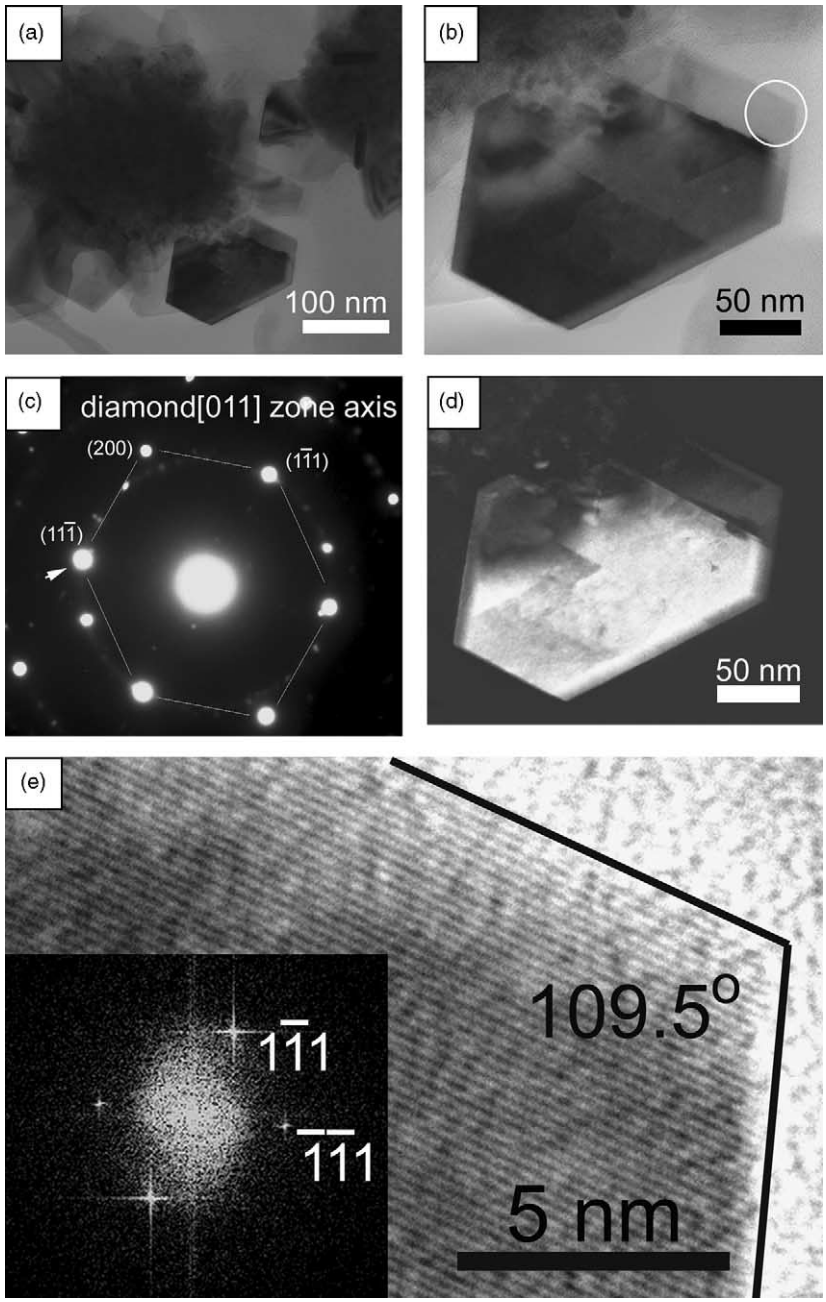

Fig. 3. (a) BF TEM image of diamond nanoplatelets; (b) an enlarged image of the hexagonal-shaped diamond; (c) electron diffraction pattern of diamond in [1 1 0] zone axis; (d) DF TEM image taking from 1 1 1 reflection; (e) HRTEM image showing the fine structure of the platelet around {1 1 1}edge region circled in (b). The inset shows the corresponding diffraction pattern by the fast Fourier transformation (FFT).

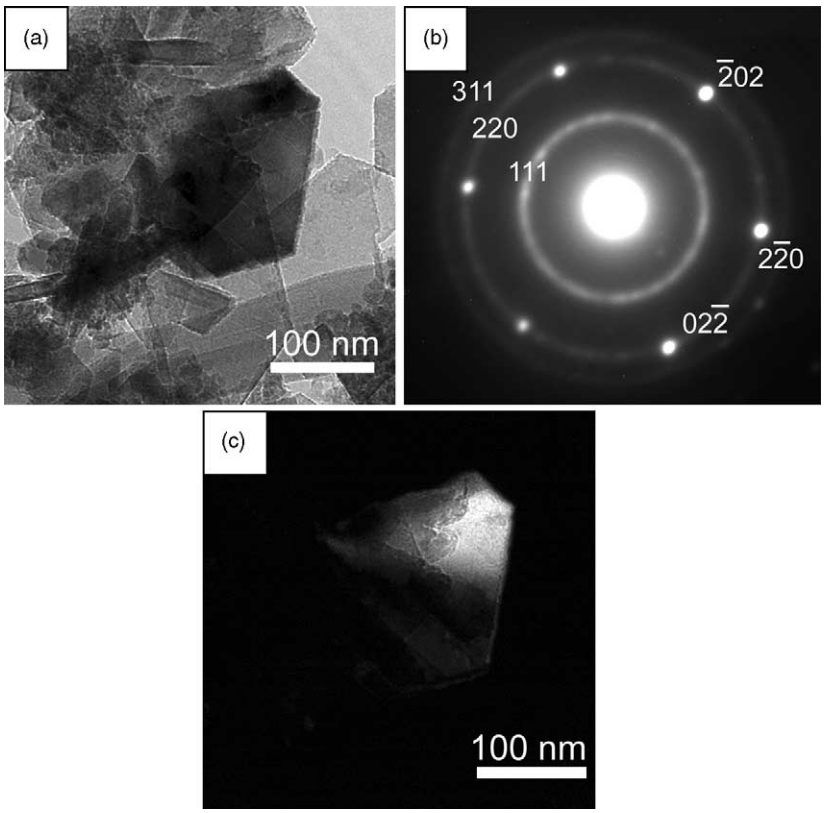

Fig. 4. (a) BF TEM image of diamond nanoplatelets; (b) electron diffraction pattern of diamond in [1 1 1] zone axis with rings; (c) DF image showing the (1 1 1) oriented diamond.

growth process. The measured temperature was over 1200 °C at the four corners and 1000 °C around the central area. The higher temperature at the corners was probably due to strong emission of secondary electrons as a result of high electric field. Therefore, it is likely that the strong bias enhances the nucleation of diamond nanoplatelets with an increased density.

3.2. Morphological and crystallographic characterization by transmission electron microscopy

The crystallographic and morphological analysis of these nanoplatelets was further accomplished by TEM. We found two different structures of diamond nanoplatelets on the TEM samples. One of the nanoplatelet has {1 1 0} tabular surface, while the other exhibits {1 1 1} face. The typical bright-field (BF) TEM image of a diamond nanoplatelet is shown Fig. 3(a). We can see that most of nanoplatelets are clustered together. Interestingly, isolated diamond platelets were observed occasionally in TEM examinations. It can be found that most of interlaced nanoplatelets are adhered to the periphery of an aggregate of nanocrystallite diamonds as shown later. From the high-magnification BF image (Fig. 3(b)), the characteristic morphology of a crystalline nanoplatelet is clearly seen in a nearly hexagonal shape with well defined facets. The average linear dimension is about 70–150 nm. It is noted that the six sides are not in equal length, but the angle between the neighboring sides is 125° and 109° which are specifically defined by the cubic crystallographic directions between ⟨1 1 1⟩ and ⟨1 1 0⟩ and between ⟨1 1 1⟩ and ⟨1 1 1⟩, respectively. Analysis of the corresponding SAD pattern in Fig. 3(c) shows that the main spots from the nanoplatelet are in a cubic diamond single crystal diffraction pattern in [0 1 1] zone axis, and some extra spots are induced from the surrounding diamonds. According to the SAD, the tabular plane can be ascribed to be {1 1 0} and the facets are normal to ⟨0 0 2⟩ and ⟨1 1 1⟩ directions. Fig. 3(d) is a dark-field (DF) image taken from of a diamond 1 1 0 reflection as pointed by the white arrow shown in Fig. 3(c). The DF image shows a complementary contrast with the BF image in Fig. 3(b), indicating that it is a hexagonal-shaped platelet. It is observed that the {1 1 1} and {0 0 2} sides of the nanoplatelet are straight. Fig. 3(e) is a high-resolution TEM image taken from an edge region as marked by white circle in Fig. 3(b). The inset is a fast Fourier transformation (FFT) pattern of the image, showing [0 1 1] zone axis diffraction pattern of diamond. Thus, the facets are atomically smooth, and can be ascribed to be $(1\,\bar{1}\,1)$ and $(\bar{1}\,\bar{1}\,1)$. Also, the image shows no planar defects and dislocations in this area, suggesting that the nanoplatelet may be of high quality.

Fig. 4(a) shows a BF image from other interlaced nanoplatelets which are with clustered together as well, similar to the distribution of nanoplatelets in Fig. 3(a) in [1 1 0]

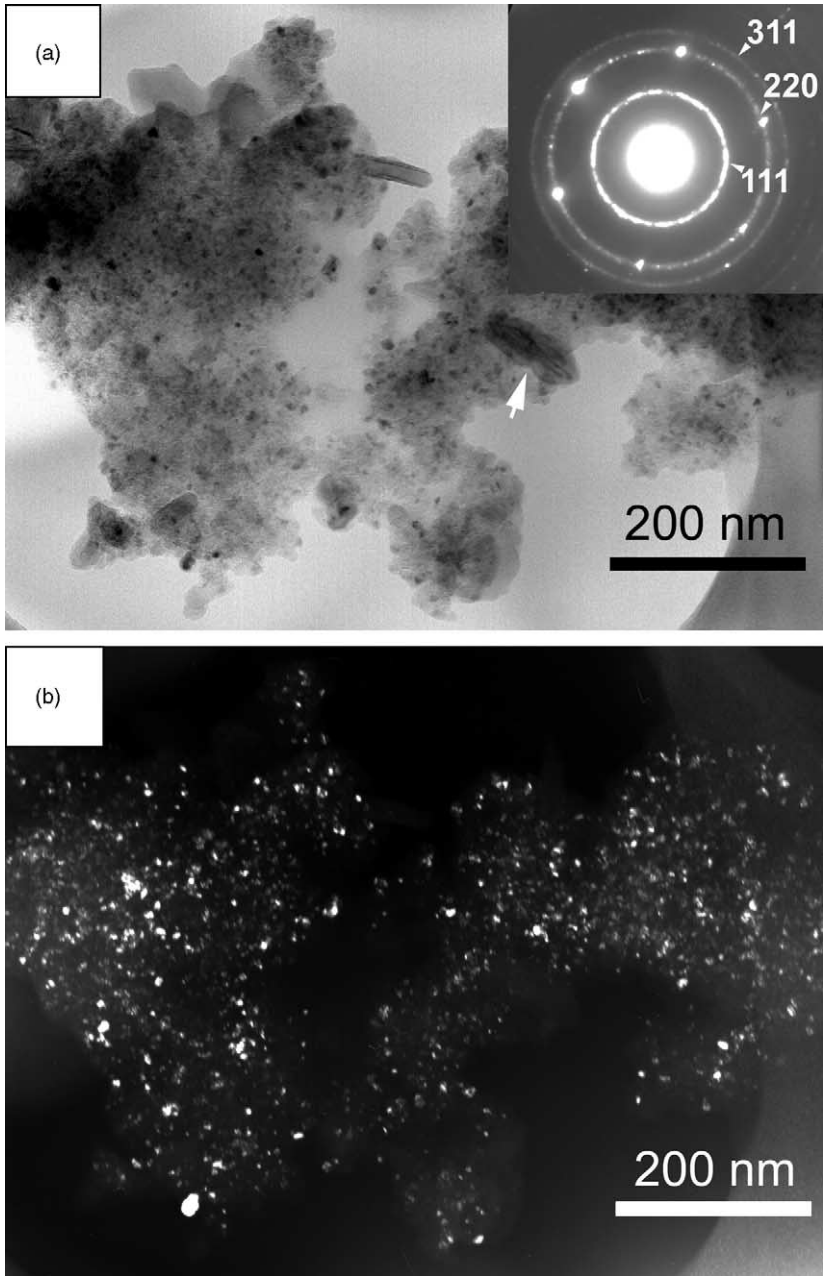

Fig. 5. (a) BF TEM image of diamond aggregates with the inset of an SAD pattern; (b) DF TEM image taking from the diamond 1 1 1 ring showing diamond nanoparticles in bright contrast.

orientation. The corresponding electron diffraction pattern in Fig. 4(b) reveals a typical single crystalline diamond reflections, however, in [1 1 1] zone axis. The rings are also identified as diamond reflections from the smaller nanodiamonds and diamond nanoplatelets. Using $\bar{2}$ 0 2 reflection for DF imaging as shown in Fig. 4(c), we can recognize that the [1 1 1] pattern is from the central diamond platelet in which the angle between the adjacent sides is 120°. Therefore, it has an orientation in [1 1 1], i.e. {1 1 1} tabular faces. It should be mentioned that ⟨1 1 1⟩ oriented diamond nanoplatelets were occasionally observed in examination of a TEM sample, it is easily found nanoplatelets in ⟨0 1 1⟩ orientation instead. Hence, it can be drawn that most of diamond nanoplatelets are ⟨0 1 1⟩ oriented.

In addition to diamond nanoplatelets, we also found that diamond aggregates are often clustered together with diamond nanoplatelets in many examinations of our TEM samples. For example, it is seen in Fig. 3(b) and (d) that the diamond nanoplatelet is bounded with other diamonds at a rough side. Fig. 5(a) is the typical BF image of an aggregate with a number of nanoplatelets. In fact, the aggregate consists of a great quantity of nanosized particles of diamond. The SAD (inset of Fig. 5(a)) exhibits cubic diamond rings in addition to the strong diffraction spots of diamond contributed from the

nanoplatelet as indicated by a white arrow. Fig. 5(b) shows the DF image taking from the diamond 1 1 1 ring. In this figure, we can see that there are many nanometer-sized diamond crystallites in bright contrast uniformly distributed in the aggregate. In detailed examination of SEM micrographs (e.g. Fig. 2(b)), it can be observed that diamond nanoplatelets seem to be stuck on aggregated nanoparticles underneath as well. We doubt that the diamond nanoparticles might the nucleation sites for diamond nanoplatelets. Further experiments are needed to clarify the growth mechanism for formation of diamond nanoplatelets.

In contrast with diamond growth in conventional MPCVD process which is in the temperature range from 700 to 900 °C and normally forms diamond crystallites in polyhedral shapes, it seems that the high temperature condition in the present case might be a proper situation to grow hexagonal-shaped diamond nanoplatelets. Similar diamond nanoplatelets have also been synthesized on various substrates in different arrangements only when the substrate temperature was higher than 1000–1200 °C [12–14].

4. Conclusions

Hexagonal-shaped diamond nanoplatelets were synthesized by MPCVD with a CH_4/H_2 gas flow ratio of 0.667% at substrate temperature over 1100 °C. Both ⟨1 1 0⟩ and ⟨1 1 1⟩ orientated diamond nanoplatelets of single crystallinity are identified. The diamond nanoplatelets have a regular shape in hexagon with a thickness about 20–30 nm and a length of several hundreds of nanometers. In addition, diamond particles with a size of several nanometers are found to be densely packed in the aggregate matter.

Acknowledgement

We thank the support from National Science Council, Taiwan, ROC, under contract of NSC92-2216-E009-020.

References

[1] E.S. Baik, Y.J. Baik, Thin Solid Films 295 (2000) 377.
[2] H. Masuda, T. Yanagishita, K. Yasui, K. Nishio, I. Yagi, T.N. Rao, A. Fujishima, Adv. Mater. 13 (2001) 247.
[3] H. Gleiter, Prog. Mater. Sci. 33 (1989) 223.
[4] D.M. Gruen, Annu. Rev. Mater. Sci. 29 (1999) 211.
[5] J.B. Wang, C.Y. Zhang, X.L. Zhong, G.W. Yang, Chem. Phys. Lett. 361 (2002) 86.
[6] T. Sharda, T. Soga, T. Jimbo, M. Umeno, Diam. Relat. Mater. 10 (2001).
[7] X. Jiang, C.L. Jia, Appl. Phys. Lett. 80 (2002) 2269.
[8] M.Q. Ding, W.B. Choi, A.F. Myers, A.K. Sharma, J. Narayan, J.J. Cuomo, J.J. Hren, Surf. Coat. Technol. 672 (1997) 94.
[9] J.B. Cui, M. Stammler, J. Ristein, L. Ley, J. Appl. Phys. 88 (2000) 3667.
[10] C. Venkatraman, C. Brodbeck, R. Lei, Surf. Coat. Technol. 115 (1999) 215.
[11] J.C. Angus, M. Sunkara, S.R. Sahaida, J.T. Glass, J. Mater. Res. 7 (1992) 3001.
[12] S.Y. Cho, Master Thesis, Department of Materials Science and Engineering, National Chiao Tung University, 2003.
[13] H.G. Chen, L. Chang, Diam. Relat. Mater. 13 (2004) 590.
[14] C.A. Lu, L. Chang, Diam. Relat. Mater. 13 (2004) 2056.